MAT JOURNALS

Journal of Electronics and Communication Systems
Volume 3 Issue 2

Design CNN On Bone Spine Segmention TO Methods Image Processing

Maysam Toghraee[1], MohammadReza Toghraee[2], M.Leena Silvoster[3], Farhad Rad[4]
[1]Department Software Computer Engineering, Science and Research, Islamic Azad University, Yasouj, Iran
Email:may.toghraee@gmail.com
[2]Department Industrial management, Sepahan Institute of Higher Education, Isfahan, Iran,
Email:mo.toghraee@gmail.com
[3]Department of Computer Science, National Institute of Technology, Calicut, Kerala, India
Email:Leenasilvoster@gmail.com
[4]Faculty of Engineering, Department of Computer Science, Islamic Azad University, Yasouj, Iran.
Email:fd_rad@gmail.com

Abstract

*This thesis proposes a deep learning approach to bone segmentation in abdominal CNN+PG. Segmentation is a common initial step in medical images analysis, often fundamental for computer-aided detection and diagnosis systems. The extraction of bones in PG is a challenging task, which if done manually by experts requires a time consuming process and that has not today a broadly recognized automatic solution. The method presented is based on a convolutional neural network, inspired by the U-Net and trained end-to-end, that performs a semantic segmentation of the data. The training dataset is made up of 21 abdominal PG+CNN, each one containing between 0 and 255 2D transversal images. Those images are in full resolution, 4*4*50 voxels, and each voxel is classified by the network into one of the following classes: background, femoral bones, hips, sacrum, sternum, spine and ribs. The output is therefore a bone mask where the bones are recognized and divided into six different classes. In the testing dataset, labeled by experts, the best model achieves a Dice coefficient as average of all bone classes of 0.8980. This work demonstrates, to the best of my knowledge for the first time, the feasibility of automatic bone segmentation and classification for PG using a convolutional neural network.*

Keywords:*Neural network; Spina Bifida Occulta; spin and ribs*

INTRODUCTION

The spine is the body of the skull, which starts from the base of the skull and extends throughout the neck and trunk. This column consists of 5 areas: 1. Cervical region, 2. Breast region, 3. Lumbar region (including 5 vertebrae), 4. Sedative area, 5.Sequence area (2 and 1).

One of the most common disorders of the spine is a back pain that can lead to lumbar disc disease; this disease is closely related to the occupation of people and is due to incorrect use of the vertebrae and the inappropriate way people behave with their body. Providing a suitable model would help a great deal of the biomechanical analysis of the spine vertebrae.

For example, many studies have been done on finite elemental modeling as a substitute for in-vitro tests on the spine. This is a reciprocating, inexpensive and configurable computing method. One of these studies shows that moderate tension in the spinal flexion is due to the resistance of the ligament ligation.[5] Other studies on the biomechanics of the spine during lifting and bending it in prayer position showed that factors such as body weight,

destination height and anthropometry affect the force on the spine (7.6).

However, studies that have been carried out using biomechanical methods and considering ergonomic issues in the work environments and anthropometrics of individuals have examined the causes of septum disturbances are less noted. For this purpose, the effect of anthropometry and ergonomics on the health of workers in work environments has been investigated in this study.

Another man, in order to design tools, machines, tasks, jobs and work environments. The goals of using this science include: improving personal productivity and improving quality, reducing injuries and providing organizational security and comfort, reducing systemic waste, reducing mistakes, and humans (10).

Failure to pay attention to the principles of ergonomics while doing work threatens the health of workers and causes many musculoskeletal disorders (11). According to the results of the research, one of the jobs that cause skeletal musculoskeletal disorders in the workers is welding (12). The disadvantages of this disorder can be the body's inappropriate condition, including severe lumbar flexion, cervical and shoulder bends, lifting devices (13, 11). It is noteworthy that the above mentioned risk factors may include the following three characteristics: (a) the presence of a malfunctioning agent, Should be considered.

- **Severity:** The effect of this feature on risk factors is high. In contrast, it should be noted that complete immobilization also contributes to the risk of high levels of stress in the body in the weld position. For example, over-working and working is effective.
- **Frequency:** The number of times a risk factor is applied within a given time period.
- **Duration:** the cycle when the worker is at risk [11].

So today, the need for ergonomic design in factories has been revealed to improve the productivity and working lives of operators and reduce fatigue and injuries of workers.

Related work

The U-Net architecture was extended to 3D implementations by Cicek et al. [17]. Their network is trained with 2D annotated slices and it generates dense volumetric segmentations. This is an interesting development of the original U-Net as a high percentage of medical data is in 3D, with similar size in each dimension, and a slide-by-slides application of 2D convolutional operations can be inefficient. Inspired by the U-Net, another volumetric, fully-convolutional neural network for 3D image segmentation was proposed by Milletari et al. [14] with the name of V-Net. The V-Net performs 3D convolutions with volumetric kernels and employs the so-called residual blocks to tackle the vanishing gradient problem. The residual block is a learning framework recently introduced in order to make the optimization process easier in image recognition tasks [18]. At the end of these blocks the signal, processed through convolutions and non-linearities, is summed with the initial input of the stage. In this way less time is required to reach convergence. In Figure 3.3 a building block of residual learning is shown. Another relevant difference of the V-Net compared to the U-Net is the objective function. The cross-entropy is indeed not used anymore and to cope with the unbalanced classes problem an objective function based on the Dice coefficient is proposed. Maximizing the dice similarity coefficient does not require any

hyperparameters (as the weight map, for example) and that is therefore an advantage of this approach. In the original study the V-Net was trained end-to-end on a dataset of prostate scans in MRI, given the relative manual ground truth annotations. It achieved a fast and accurate segmentation based on the Dice coefficient.

In addition, it is worth mentioning a brand new segmentation approach based on adversarial training. Good fellow et al. [20] introduced in 2014 generative adversarial networks, a new framework for estimating generative models via an adversarial process. Here two networks are trained simultaneously, one that generates data and one that learns to determine whether a sample comes from the training data or the generative model. The competition between the two models drives the generative network to improve its results, producing data that the discriminative model cannot distinguish from the original one. Recently, adversarial networks have been introduced also for semantic segmentation [21]. This framework has proved to be effective to correct inconsistencies between the ground truth and the segmentation map produced by a segmentation CNN. This approach has achieved interesting results in the medical imaging field regarding the segmentation of prostate cancer in MRI [22] , organs in chest X-Rays [23] and brain MRI [24]. All those studies show segmentation performance improvements compared to previous methods based on a single segmentation net. A further investigation of this framework, also regarding different tasks, represents an interesting deep learning topic of research of the future. To conclude, in the last years various medical image segmentation tasks have been tackled with different deep learning approaches. The ones receiving as input the whole image or a large sub region have been prevailing over the "CNN+PG" methods, but both can be improved and not always designing a custom architecture for the specific task has turned to be the only optimal solution.

BS segmentation using CNN and PG via a graph cut

Proposed approach

In this work, we have automated use of the learner's machine, which calculates the interlacing neural network algorithm with the method of image processing. This learner machine is trained and uses the sum of the images taught by the segments produced and the experiences of the related experts.

This graphic learner cnn can display the effect of the segments with any image partition that is loaded. CNN is updated to a new conversation through learner processing; it has the ability to automatically extract the limited photos.

We propose a new method for solving the problem of group problem using the CNN combination and the procedure of dialogic groups through video processing. In this algorithm, the pixel classification is only through the Random F_VALUE and the use of component parts productivity. Probably one member estimates a local estimate using the predicted rendom. Global productivity has had a beneficial impact on minimal graphic productivity.

According to well-conducted studies, the use of algorithm segments; which calculates the rotational distance between the two edges of the However; the two decision edges for a good conversation; the output of these edges is the inadequate defining of these groups.

These studies are within the influence of the graphic generated from conversational neural networks by spinal image using graphical image partition and effective efficiency on this algorithm. The goal is to minimize the cost between these images.

Convolutional neural network

The learning architecture of a learning machine like the interactive neural network is the automatic method of initiating an effective prediction of the function. CNN is a multi-layer perceptron designed to detect a two-dimensional shape, with high precision transmissions, and calculates the scale, Dice, and other characteristics. and calculates the advantage of the CNN; CNN is able to provide a new position for training data and can detect test data

.

The CNN advantage does not require image preprocessing, and CNN contains a series of top layers, each layer containing one or more layouts.

CNN is able to recognize the features associated with the trained data set. The efficiency of this algorithm depends on the functions. In this paper, the functionality of the function affects the perceptron group.

Using these weights in perceptron itself affects the conversational neural network algorithm, and sharing these weights helps to reject a number of free parameters. Composing free parameters on the network is a good use for disseminating learner data.

Neural Networks Defend Graphic Directing. These nodes are repeatedly presented in CNN. The voids are filtered, and the weights of these edges are shared between images, and according to observations of the weights and the number of nodes Their total weight is chosen as a priority.

Initialization of CNN

Each layer of CNN is used in the contents of the 6 properties that are non-linear. These CNN filters are sized 5x5. The effect of categorizing these images 17 * 17 groups of images has been created for edges. The choice of random weights is achieved by element elements with a normal distribution of standards.[28].

Learning algorithm

This batch of processing for each update is guaranteed, computed and ultimately trained. In this method, the algorithm shows the speed of the speed of the interactive networks. So we use online learning for this problem. So, using this algorithm, according to the weights defined in the layers of the perceptrons, provides the minimum possible cost for these nodes with respect to the defined threshold, and the neural network interpolates the order of the operators using the linear and nonlinear filters Is.

The input data for this BS image and the output of these layers consists of two images. While alternative layers include (referenced layers and hidden layers) that include images that invoke the properties map. Character Map Calculates the data input of this algorithm. Neural Network The interactive collaboration of the graphs on the nodes of the grid is obtained through experiments. In layers, each layer of 5 × 5 has six attributes, and the categories are 17 * 17 for each edge. GetsThe input data of this spatial algorithm of nerve networks detects the number of rows and attributes by CNN, and the outputs of CNN give two images of the edges of x and y.

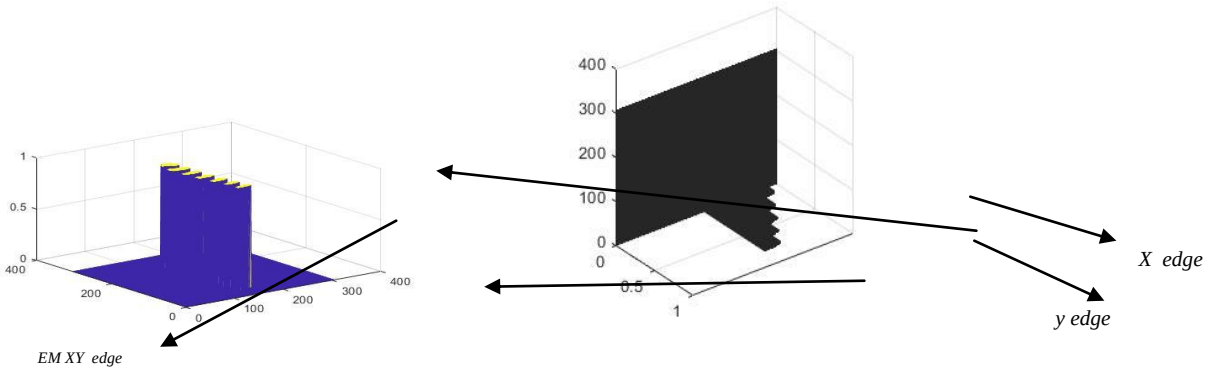

Fig. 1.*Convolutional neural network*

The input of the Convolutional Neural Network is the raw input image and the features of the image are automatically detected by CNN. CNN is learned using online stochastic gradient descent learning algorithm and it is adapted to new environments. The output of the CNN gives two images, x edge and y edge. Using an affinity function, the affinity graph is constructed.

Perceptual grouping constraints via a graph cut

The input data for this BS image and the output of these layers consists of two images. While alternative layers include (referenced layers and hidden layers) that include images that invoke the properties map. Character Map Calculates the data input of this algorithm. Neural Network

The interactive collaboration of the graphs on the nodes of the grid is obtained through experiments. In layers, each layer of 5 × 5 has six attributes, and the categories are 17 * 17 for each edge. Gets

The input data of this spatial algorithm of nerve networks detects the number of rows and attributes by CNN, and the outputs of CNN give two images of the edges of x and y.

As you can see in the figure, there is a source node whose function is to exchange useful and raw information to other nodes, and each node is connected by the edges, each of these edges having a definite weight, the node weighing It is less for prioritized to the output. Each of them has a specific sink that performs its exchange of information through a sink or network, as shown below:

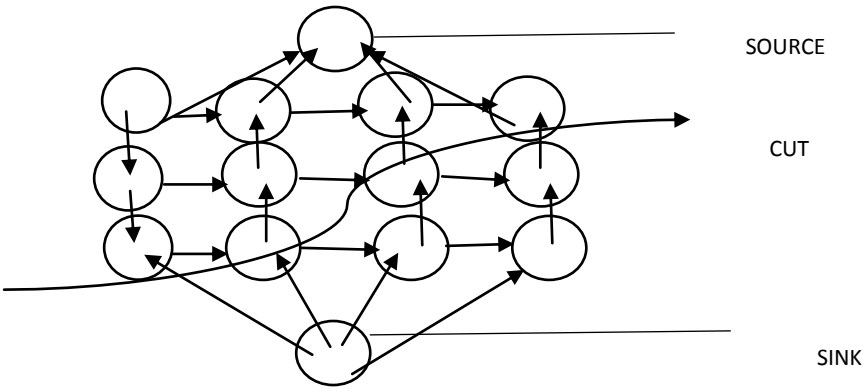

Fig. 2. *Graph cut*

Labeling of pixels is done in such a way that optimizes the energy function E(y). E(y) is formulated as [13]:

$$E(Y) = \sum_{P \in P} E_d(y)_p \quad + \gamma \sum_{p \in \rho, q \in n_c(p)} E_s(y_p, y_q) \qquad (1)$$

Where, $E_d(y)_p$ is a data term and $E_s(y_p, y_q)$denotes the smoothness term. P is the set of all pixels in the raw EM and $n_2(p)$ is the set of all pixels adjacent to a pixel p in the 2D image plane. However, for efficient segmentation we need to modify this terms.

The global minimum of E(y) can be computed by max-flow/min-cut algorithm. In order to reduce the discontinuities in the segmentation for neighboring pixelsE_s is redefined as [13]:

$$E_s(y_p, y_q) = exp\left(-\frac{(x_p - x_q)^2}{2\partial_s^2}\right).\frac{\partial(y_p - y_q)}{dist(p,q)} \qquad (2)$$

Where, $x_p$is the gray value of the image at pixel p and q)dist(p, q is the distance between the neighboring pixels.

Kronecker delta function ensures that the energy term is regular. Probabilistic output of the random forest classifier is used for membrane detection. In order to minimize the computational cost, histograms over the context region are taken. In order to eliminate the false positive of the segmentation, principle of good continuation to close the gaps along membrane is used. A directional energy is introduced to avoid the shortcomings of the gradient flux so that smoothness in labeling is ensured.$E_{gc}$is formulated as [13]:

$$E_{gc}(y_p, y_q) = |< v_p - v_{pq} >| . exp\left(-\frac{(x_p - x_q)^2}{2\partial_s^2}\right).\frac{\partial(y_p - y_q)}{dist(p,q)} \qquad (3)$$

Where, v_{pq} is the unit vector with orientation of the straight line between pixels p and q, and v_p is a vector directed along the membrane. The smoothness along the direction of the membrane pixels are overcome by E_{gc} .

To incorporate information from adjacent sections into the segmentation,$E_{na}$is defined as [13]:

$$E_{na}(y_p, y_q) = m_q . |< v_p - v_{pq} >| . \frac{\partial(y_p - y_q)}{dist(p,q)} \qquad (4)$$

Where, m_q is the probability of pixel q on the membrane andv_p is the largest eigenvector of the Hessian at pixel p multiplied by the corresponding eigenvalue. Since the effect of gradient flux is minimum (false positive membrane segmentation) due to the texture in the image, we omit the gradient flux and the final energy term is formulated as[13]:

$$E(Y) = \sum_{P \in P} E_d(y)_p \quad + \gamma \sum_{p \in \rho, q \in n_2(p)} E_s(y_p, y_q) + \partial_{gc} \sum_{p \in \rho, q \in n_2(p)} E_{gc}(y_p, y_q) + \partial_{na} \sum_{p \in \rho, q \in n_3(p)} E_{na}(y_p, y_q) \qquad (5)$$

Where, $E(Y)$ is the energy term. The first term denotes the energy term of the probabilistic output of the random forest classifier for every pixel p∈P. The second term denotes the directional energy term based on good continuation.$n_2(p)$, denotes the set of all pixels adjacent to a pixel q in the 2D image plane. The third term denotes the energy of the smoothness term. $n_3(p)$is the set of neighboring pixels in adjacent section (3 dimension). The fourth energy term incorporates images from the adjacent sections [13].

Convolutional Neural Network constructs the affinity graph which is segmented using perceptual grouping constraints via a graph cut. In the first phase, affinity graph is generated using CNN. The second phase of the proposed method consists of two steps: construction of a graph from the perceptual grouping, and then partition the graph according to max-flow min-cut theorem. The first step includes a mapping of the perceptual grouping problem to an energy function. A cue evaluation algorithm for each feature pair is computed. The second step uses graph cuts to minimize the cost function to find the "preferred" perceptual groups. The probability output of a random forest classifier is used in a regular cost function, which integrates the information available from gap completion via perceptual grouping constraints. The segmentation is posed as a minimization of the regular cost function involving the image intensity and the flux of the intensity gradient field, and graph cut is used to compute the globally optimal solution.

The computation of the minimum cut can be efficiently performed by the max flow algorithms. In past studies, Minimum cut algorithms principle has been applied to a wide range of problems. The energy term is regular and can be globally optimized using max-flow/min-cut computation. Label each pixel in p ∈ P with {0,1} such that the labels for all pixels minimizes the Energy term E(y) defined in (5) (see Algorithm 1).

Algorithm 1. Perceptual grouping constraints via a graph-cut [13]

Step 1. Given an image, construct a graph g=(v,e) and the weights of the edges are the similarity between pixels.

Step 2. For all nodes p=p ,$n_2(p)$

$$E(Y) = \sum_{P \in P} E_d(y)_p + \gamma \sum_{p \in \rho, q \in n_2(p)} E_s(y_p, y_q) + \partial_{gc} \sum_{p \in \rho, q \in n_2(p)} E_{gc}(y_p, y_q) + \partial_{na} \sum_{p \in \rho, q \in n_3(p)} E_{na}(y_p, y_q) \ .$$

Step 3. Check whether entire labeling y for all pixels minimizes the energy function; if yes − terminate, otherwise go to Step 2.

Although this energy term incorporates information from adjacent sections, the main focus of the segmentation is two dimensional. This is due to the fact that the resolution of SEM images is high (about 5 nm per pixel), but along the vertical direction of the image stack, the resolution is limited by the section thickness of the sample [13].

The algorithm proposed

The perceptron structure of the groups introduces the PG algorithm to obtain a shear graph [13]. When combined with neural networks, they increase the efficiency of the algorithm. The energy effect of the graph is obtained from the efficiency of the perceptron groups to achieve the shear graph. CNN algorithm the graphical effect of a very effective graph is generated when PG does not provide useful information. PG + CNN come with this information and provide useful and healthy information and

improve the functionality of this algorithm.

Algorithm 2. Proposed method

Phase1: CNN

Step 1. Input the raw SEM image and the ground truth image into the CNN.

Step 2. Update the weights in the network until the x-edges and y-edges are correctly classified.

Step 3. Construct a graph from the above edge image.

Phase 2: PG

Step 1. The output of CNN is considered as the input of PG algorithm.

Step 2. Cost function is optimized as (5).

Step 3. Output of this algorithm is the segmented image.

Performance evaluation and results

Performance evaluation

The performance of various schemes suggested is evaluated using the popular precision, recall, true positive rates, false positive rates, accuracy and F-score measures, whose standard definitions are as given below: Precision (Pr). This is the ratio of the true positives to the sum of true positives and false positives:

$$pr = \frac{TP}{TP + FP}$$

Recall (Re). This is the ratio of true or actual positives to the sum of actual positives and false negatives.

$$Re = \frac{TP}{TP + FN}$$

These two measures, precision and recall, quantitatively represent the quality of segmentation algorithms irrespective of whether the image is over segmented or under segmented.

Precision tells us what fraction or percent of the algorithm detected boundary pixels are the boundary pixels in the ground truth. This measure is sensitive to over segmentation. Recall tells us the fraction or percent of the ground truth boundary pixels that are detected by the algorithm. This percent is sensitive to under segmentation. F-score is defined as the harmonic mean of the precision and the recall.

$$F\_Score = \frac{2 * pr * Re}{pr + Re}$$

Other related measures are False Positive Rate (FPR), True Positive Rate (TPR) and Accuracy. FPR is defined as the ratio of the false positives to the sum of false positives and false negatives. This measure denotes the correctly classified portion of the positives events.

$$FPR = \frac{FP}{FP + TN}$$

TPR is defined as the ratio of true positives to the sum of true positives and true negatives. It denotes the positive outcome fraction of the total absent events.

$$TPR = \frac{TP}{TP + FN}$$

Accuracy is defined as the ratio of the misclassified pixels to the total number of pixels.

$$Accoracy = \frac{TP + FN}{TP + FN + TN + FP}$$

Where, TP, FP, TN and FN respectively denote the number of true positive, false positive, true negative and false negative predictions. We demonstrate the training of Convolutional Neural Network (CNN) to produce an affinity graph from raw BS images. We are able to correctly predict the affinity graph when perceptual grouping constraints via a graph cut (PG) is combined with the output of Convolutional Neural Network. Then, in the post processing step, contour of the image is detected and it is added to the image. F-Value of this proposed work is obtained as 0.8980.

Data set

We used the data collection in Warflyla, the first bone marrow donor database with a series of spinal column (SBM) SBM images, to provide an effective resolution

and complete compilation of complete neural discussions. A stack contents image to several thousand images with a complexity of measuring 2 * 2 * 15 cells estimated with a source of 4 * 4 * 50 pixels [29]. Nonlinear lens of the electromagnetic lens is used for pre-processing modification. Several image cells have been used for Z-Alignment performance. An accurate image preprocessing of image j [30] was used to properly use the damaged beads to reduce the gap between the vertebrae of the spine.

Experimental results and discussion

The input image is given in Fig. 3. Ground truth Image in two forms is as shown in Fig. 4. The output of perceptual grouping via graph cut (PG) algorithm is shown in Fig. 5a, and the output of proposed approach (PG combined with CNN) is given in Fig. 5b.

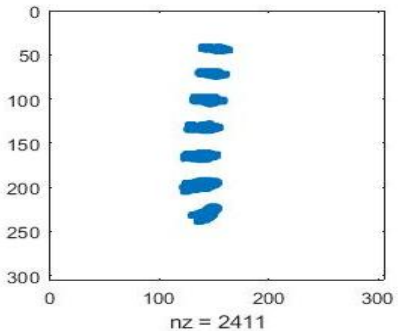

Fig. 3.*Input image*

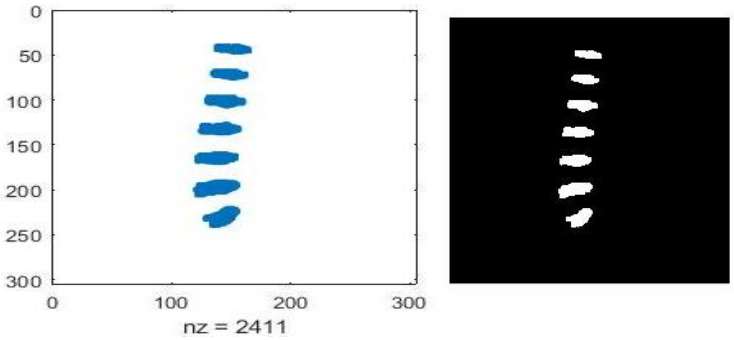

Fig. 4.*Ground truth*

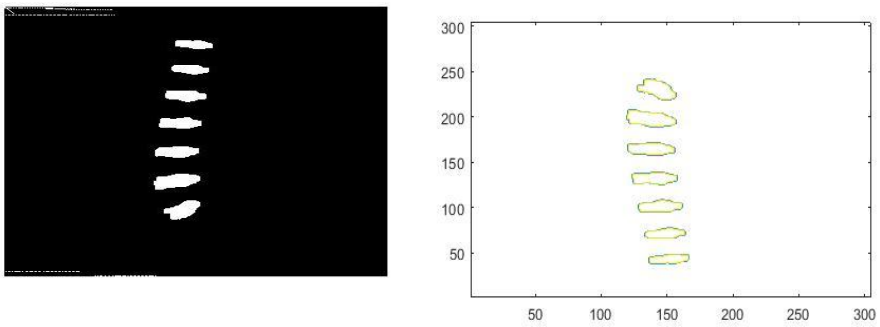

a – Output of PG b – output of PG+CNN

Fig. 5.*Results of segmentation*

The image shows the color overlay of the segmentation with good continuation and the ground-truth label.

False positives are shown in green and false negatives are shown in red. The results in the form of quantitative measures of evaluations are given in Table 1 for PG and PG+CNN.

Table 1.*Comparison of results*

Method	Precision	Recall	Accuracy	F-Value	Dice
PG	0.8920	0.9042	0.9947	0.8980	0.8980
PG+CNN	0.89198	0.90419	0.99468	0.89804	0.89804

The segmentation performance measures of the proposed approach, CNN+PG, are compared with the perceptual grouping constraints via a graph cut (PG) 96 approach. The results demonstrate that the precision and the F_Value are highest for the proposed approach, and the other measures are also improved in the proposed approach. The experimental studies demonstrate also that the computational time is reduced as compared to the purely manual tracing algorithms.

CONCLUSION

In this paper, using a PG method and another method of PG + CNN, two methods were used. When we call the input data, we saw with PG that the efficiency of the images has not changed to improve the spin-gap efficiency. The second method, PG + CNN, has been used. Performance in Table 1, we can see how much the distance between the spins Lower and improved the efficiency and accuracy of the spine, which has calculated the value of this F_Value procedure.

REFERENCES

1. Ian Goodfellow, YoshuaBengio, and Aaron Courville. Deep Learning. MIT Press, 2016. http://www.deeplearningbook.org.
2. Geert Litjens, ThijsKooi, BabakEhteshamiBejnordi, Arnaud ArindraAdiyosoSetio, Francesco Ciompi, Mohsen Ghafoorian, Jeroen AWM van der Laak, Bram van Ginneken, and Clara I Sánchez. A survey on deep learning in medical image analysis. arXiv preprint arXiv:1702.05747, 2017.
3. U l l m a n, S., A. S h a s h u a. Structural Saliency: The Detection of Globally Salient Structures Using Locally Connected Networks. – In: Proc. ICCV-88, 1988, 321-332.
4. G u t f i n g e r, D., J. S k l a n s k y. Robust Classifiers by Mixed Adaptation. – Pattern Analysis and Machine Intelligence, Vol. 13, 1991, 552-566.
5. G u y, G., G. M e d i o n i. Perceptual Grouping Using Global Saliency-Enhancing Operators. – In: Proc. International Conference on Pattern Recognition, IEEE, Vol. 1, 1992, 99-103.
6. M o n t e s i n o s, P., L. A l q u i e r. Perceptual Organization of Thin Networks with Active Contour Functions Applied to Medical and Aerial Images. – In: Proc. Vienna International Conf. on Pattern Recognition, IEEE, 1996, 647-651.
7. S h a s h u a, A., S. U l l m a n. Grouping Contours by Iterated Pairing Network. – In: Advances in Neural Information Processing Systems, Vol. 3, 1990, 335-341.
8. P a r e n t, P., S. W. Z u c k e r. Trace Interface, Curvature Consistency, and Curve Detection. – In: Pattern Analysis and Machine Intelligence, Vol. 11, 1989, 823-839.
9. C l e m e n s, D. T. Region-Based Feature Interpretation for Recognizing 3D Models in 2D Images. –Ph. Dissertation, MIT, 1991.
10. L e u n g, T., J. M a l i k. Detecting, Localizing and Grouping Repeated Scene Elements from an Image. – In: Computer Vision-ECCV, Vol. 1, 1996, 546-555.
11. M a c k e, J. H., N. M a a c k, R. G u p t a, W. D e n k, B. S c h o l k o p f, A. B o r s t. ContourPropagation Algorithms for Semi-Automated

Reconstruction of Neural Processes. – Journal of Neuroscience Methods, Vol. 167, 2008, No 2, 349-357.
12. G r o s s b e r g, S., E. M i n g o l l a. Neural Dynamics of Perceptual Grouping: Textures, Boundaries, and Emergent Segmentations. – Attention, Perception, & Psychophysics, Vol. 38, 1985, No 2, 141-171.
13. B e c k, J. Effect of Orientation and of Shape Similarity on Perceptual Grouping. – Attention, Perception, & Psychophysics, Vol. 1, 1966, No 5, 300-302.
14. K a y n i g, V., T. F u c h s, J. M. B u h m a n n. Neuron Geometry Extraction by Perceptual Grouping in Sstem Images. – In: IEEE Conference on Computer Vision and Pattern Recognition (CVPR), IEEE, 2010, 2902-2909.
15. FaustoMilletari, Nassir Navab, and Seyed-Ahmad Ahmadi. V-net: Fully convolutional neural networks for volumetric medical image segmentation. arXiv preprint arXiv:1606.04797, 2016.
16. Alex Fedorov, Jeremy Johnson, EswarDamaraju, Alexei Ozerin, Vince Calhoun, and Sergey Plis. End-to-end learning of brain tissue segmentation from imperfect labeling. In Neural Networks (IJCNN), 2017 International Joint Conference on, pages 3785–3792. IEEE, 2017.
17. YangqingJia, Evan Shelhamer, Jeff Donahue, Sergey Karayev, Jonathan Long, Ross Girshick, Sergio Guadarrama, and Trevor Darrell. Caffe: Convolutional architecture for fast feature embedding. arXiv preprint arXiv:1408.5093, 2014.
18. ÖzgünÇiçek, Ahmed Abdulkadir, Soeren S Lienkamp, Thomas Brox, and Olaf Ronneberger. 3d u-net: learning dense volumetric segmentation from sparse annotation. In International Conference on Medical Image Computing and Computer-Assisted Intervention, pages 424–432. Springer, 2016.
19. Kaiming He, Xiangyu Zhang, ShaoqingRen, and Jian Sun. Deep residual learning for image recognition. In Proceedings of the IEEE conference on computer vision and pattern recognition, pages 770–778, 2016
20. PimMoeskops, Jelmer M Wolterink, Bas HM van der Velden, Kenneth GA Gilhuijs, Tim Leiner, Max A Viergever, and IvanaIšgum. Deep learning for multi-task medical image segmentation in multiple modalities. In International Conference on Medical Image Computing and Computer-Assisted Intervention, pages 478–486. Springer, 2016.
21. Ian Goodfellow, Jean Pouget-Abadie, Mehdi Mirza, Bing Xu, David Warde-Farley, SherjilOzair, Aaron Courville, and YoshuaBengio. Generative adversarial nets. In Advances in neural information processing systems, pages 2672–2680, 2014.
22. Pauline Luc, Camille Couprie, SoumithChintala, and JakobVerbeek. Semantic segmentation using adversarial networks. arXiv preprint arXiv:1611.08408, 2016.
23. Simon Kohl, David Bonekamp, Heinz-Peter Schlemmer, KaneschkaYaqubi, Markus Hohenfellner, Boris Hadaschik, Jan-Philipp Radtke, and Klaus Maier-Hein. Adversarial networks for the detection of aggressive prostate cancer. arXiv preprint arXiv:1702.08014, 2017.
24. Wei Dai, Joseph Doyle, Xiaodan Liang, Hao Zhang, Nanqing Dong, Yuan Li, and Eric P Xing. Scan: Structure correcting adversarial network for chest x-rays organ segmentation. arXiv preprint arXiv:1703.08770, 2017.
25. PimMoeskops, MitkoVeta, Maxime W Lafarge, Koen AJ Eppenhof, and Josien PW Pluim. Adversarial training

and dilated convolutions for brain mri segmentation. In Deep Learning in Medical Image Analysis and Multimodal Learning for Clinical Decision Support, pages 56–64. Springer, 2017.
26. Lee W Goldman. Principles of ct and ct technology. Journal of nuclear medicine technology, 35(3):115–128, 2007.
27. Toghraee M, rad F, parvin H,.(2017). *The Influence Select Feature on The Clustering Algorithm*. Journal of Computer Science Engineering and Software Testing Volume 3 Issue 3.pp:1-10.
28. C a r d o n a, A., S. S a a l f e l d, S. P r e i b i s c h, B. S c h m i d, A. C h e n g, J. P u l o k a s, P. T o m a n c a k, V. H a r t e n s t e i n. An Integrated Micro and Macroarchitectural Analysis of the Drosophila Brain by Computer-Assisted Serial Section Electron Microscopy. – PloSBiol, Vol. **8**, 2010, No 10, e1000502.
29. C a r d o n a, A. TrakEM2: An ImageJ-Based Program for Morphological Data Mining and 3d Modeling. – In: Proc. Imagej User and Developer Conference, 2006.
30. N o w l a n, S. J., J. C. P l a t t. A Convolutional Neural Network Hand Tracker. – Advances in Neural Information Processing Systems, Vol. **7**, 1995, 901-908.
31. W ai b e l, A., T. H a n a z a w a, G. H i n t o n, K. S h i k a n o, K. J. L a n g. Phoneme Recognition Using Time-Delay Neural Networks. – In: IEEE Trans. Speech and Signal Processing, Vol. **37**, 1989, No 3, 328-339.